Acta of Bioengineering and Biomechanics
Vol. 19, No. 3, 2017

Original paper
DOI: 10.5277/ABB-00682-2016-03

A computational evaluation of sedentary lifestyle effects on carotid hemodynamics and atherosclerotic events incidence

MARIA VITTORIA CARUSO[1, 2]*, RAFFAELE SERRA[1, 3], PAOLO PERRI[1], GIANLUCA BUFFONE[4], FRANCESCO GIUSEPPE CALIÒ[4], STEFANO DE FRANCISCIS[1, 3], GIONATA FRAGOMENI[1]

[1] Department of Medical and Surgical Sciences, "Magna Graecia" University, Viale Europa, Catanzaro, Italy.
[2] Department of Mechanical, Energetic and Management Engineering, University of Calabria, Rende, Italy.
[3] Interuniversity Center of Phlebolymphology, "Magna Graecia" University, Viale Europa, Catanzaro, Italy.
[4] Operative Unit of Vascular Surgery, "S. Anna Hospital", Viale Papa Pio X, Catanzaro, Italy.

Purpose: Hemodynamics has a key role in atheropathogenesis. Indeed, atherosclerotic phenomena occur in vessels characterized by complex geometry and flow pattern, like the carotid bifurcation. Moreover, lifestyle is a significant risk factor. The aim of this study is to evaluate the hemodynamic effects due to two sedentary lifestyles – sitting and standing positions – in the carotid bifurcation in order to identify the worst condition and to investigate the atherosclerosis incidence. *Methods*: The computational fluid dynamics (CFD) was chosen to carry out the analysis, in which *in vivo* non-invasive measurements were used as boundary conditions. Furthermore, to compare the two conditions, one patient-specific 3D model of a carotid bifurcation was reconstructed starting from computer tomography. Different mechanical indicators, correlated with atherosclerosis incidence, were calculated in addition to flow pattern and pressure distribution: the time average wall shear stress (TAWSS), the oscillatory shear index (OSI) and the relative residence time (RRT). *Results*: The results showed that the bulb and the external carotid artery emergence are the most probable regions in which atherosclerotic events could happen. Indeed, low velocity and WSS values, high OSI and, as a consequence, areas with chaotic-swirling flow, with stasis (high RRT), occur. Moreover, the sitting position is the worst condition: considering a cardiac cycle, TAWSS is less than 17.2% and OSI and RRT are greater than 17.5% and 21.2%, respectively. *Conclusions*: This study suggests that if a person spends much time in the sitting position, a high risk of plaque formation and, consequently, of stenosis could happen.

Key words: *sedentary lifestyle, sitting, standing, computational fluid dynamics (CFD), carotid bifurcation, atherosclerosis*

1. Introduction

Some heart diseases and stroke are caused by atherosclerosis, generating about 50% of all deaths [14]. Its lesions occur in particular susceptible sites, characterized by complex geometry as branch points, bifurcations, and major curves [7]. Typical regions in which these lesions appear and progress are the coronary arteries, the abdominal aorta and carotid bifurcations [5]. Multiple risk factors have been identified, such as smoke, diabetes, hypertension, obesity and lifestyle [5]. Regarding the last one, moderate and vigorous exercises are associated with important decreases in the incidence of cardiovascular events, whereas sedentary lifestyle, which includes both prolonged sitting and standing times, increases cardiovascular pathologies [11].

Since the carotid arteries provide blood to the brain and since they are highly prone to the lesion formation [5], which can cause stroke, the carotid bifurcation has been considered in different studies investigating

* Corresponding author: Maria Vittoria Caruso, Bioengineering Group, Department of Medical and Surgical Sciences, "Magna Graecia" University, viale Europa, 88100 Catanzaro, Italy. Phone: +3909613694961, e-mail: mv.caruso@unicz.it
Received: June 24th, 2016
Accepted for publication: September 16th, 2016

the effects due to the hemodynamic profile generated by sedentary positions. A comparison of velocity in the carotid artery in young, middle-aged and older groups has shown that regular aerobic exercise increases values in respect to sedentary lifestyle [1]. Moreover, physical inactivity affects also the carotid intima media thickness (IMT) [9] and the carotid stiffness. Furthermore, Krause et al. [10] have found that prolonged standing at work is correlated with an increase of IMT in the carotid bifurcation. Standing and sitting positions have been investigated and compared considering the brachial and femoral arteries [18]. This study has shown that the heart rate and flow rate are higher and the mean arterial pressure (MAP) is lower in both arteries.

Although sedentary lifestyle has been investigated much from clinical viewpoint, no validated and comprehensive studies have been carried out regarding the real role of hemodynamics and its implication to atherogenesis in the carotid bifurcation in sitting and standing positions. Indeed, Malek et al. [15] have highlighted the correlation of atherosclerosis with hemodynamics, reporting that atherosclerotic lesions preferentially involve areas with blood flow recirculation and stasis, and, so, with the low wall shear stress (WSS).

The aim of this study is to explore the hemodynamic changes in the carotid bifurcation due to sedentary lifestyle considering prolonged sitting and standing times by means of the computational fluid dynamics (CFD). This numerical approach allows to analyze the two hemodynamic variables -the pressure field and the velocity pattern-in time and space resolving the governing equations by means of simulations [23]. Recently, different researchers have used CFD tools to solve complex problems and to assist in predicting the behavior of blood flow in the human body [2], [4], [12], [17], [19]. Furthermore, to compare the two sedentary conditions from a hemodynamic point of view, only one patient-specific 3D model of a carotid bifurcation was reconstructed starting from computer tomography (CT). Non-invasive pressure and velocity measurements were acquired *in vivo* in a cohort of 150 volunteers and used as input data for all simulations. To investigate the incidence of atherosclerotic events, three different parameters arising from WSS were numerically evaluated.

2. Materials and methods

2.1. *In vivo* data

This study was approved by the Investigational Review Board (IRB) of Interuniversity Center of Phlebolymphology (CIFL) International Research and Educational Program in Clinical and Experimental Biotechnology, in accordance with the Declaration of Helsinki and the Guidelines for Good Clinical Practice. Before the beginning of the study, all participants provided a written informed consent.

The subjects were 150 healthy volunteers, 77 males and 73 females, which had no cardiovascular and atherosclerotic diseases. The cohort of individuals aged 60 ± 8 years and had a body mass index (BMI) of 26 ± 3. Moreover, they were divided in two groups, according to the type of working lifestyle, established considering the working hours (generally, 8 hours) per day:

- sitting workstation – Case A: >5 hours in sitting position,
- standing workstation – Case B: >5 hours in standing position.

The information regarding the cohort is reported in Table 1.

Velocity waveforms after 1 h of sitting position and after 1 h of standing position were recorded in the external and internal carotid arteries (ECA and ICA) by means of duplex ultrasound systems. The applanation tonometry was used to record pressure in the common carotid artery (CCA). For both velocity and pressure distributions over time and for both sitting and standing groups, the mean value was evaluated for each instant, considering the hemodynamic value of each person in the group, in order to obtain mean velocity and mean pressure waveforms for each group.

Table 1. Cohort information

	Cohort	Sitting workstation	Standing workstation
Number	150	78	72
Age	60 ± 8	59 ± 4	61 ± 8
Sex	77 males – 73 females	40 males – 38 females	37 males – 35 females
BMI	26 ± 3	28 ± 1	25 ± 9

2.2. Geometrical model

As reported by Friedman et al. [6], human bifurcation geometry is sufficient to cause significant variability in the hemodynamic shear stress, which is correlated to the atherogenic process. For this reason, since the aim of the study is to compare the two sedentary lifestyle conditions and to evaluate the effects on different atherosclerotic indicators, in this study only one carotid bifurcation geometry was considered, as in a similar study [17]. Thus, in order to analyze only the effects on flow of lifestyle without taking into account the influence of vessel morphology, the same carotid bifurcation was considered as geometry in the CFD modeling of the two sedentary conditions.

A 3D real patient-specific bifurcation model of a 60-year-old healthy man who had not atherosclerotic diseases was obtained from a series of *in vivo* contrast-enhanced axial CT-scan 2D-slices, done for clinical reasons. The Toshiba Aquilion RXL CT-scan machine was used. The geometrical model was obtained by means of the imaging segmentation and the 3D reconstruction processes of the DICOM images using Invesalius, a free software. Subsequently, since the segmentation software provides a stereolithographic file (stl format), in order to obtain a good surface quality and a low number of faces, 3D mesh geometry was subjected to reverse engineering process using Geomagic products. So, the mesh was smoothed, tips were removed, holes were closed and normals were made uniform. The 3D final model consisted of 200 Nurbs surfaces (Fig. 1) and included the common carotid artery (CCA), the internal carotid artery (ICA) and the external carotid artery (ECA). All geometrical dimensions are reported in Table 2. Furthermore, in order to verify whether the computational domain respects the original medical data, all geometrical dimensions were compared with those obtained with the duplex ultrasound system – the calibers were evaluated from intima to intima (Table 2, *in vivo* data). The results indicate that the reconstruction does not significantly alter the dimensions (Table 2, error).

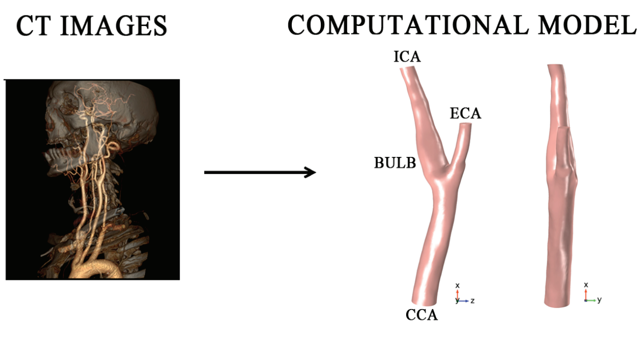

Fig. 1. The patient-specific carotid bifurcation model. Note that the second image of vessel is obtained with a turn of 90 degrees clockwise

Table 2. Patient-specific carotid bifurcation geometrical dimensions

	In vivo data		Computational model		Error	
Vessel	Caliber [mm]	Length [mm]	Caliber [mm]	Length [mm]	Caliber [%]	Length [%]
CCA	7.1	41.0	7.0	41.2	1.41	0.49
ECA	3.2	13.4	3.3	13.3	3.12	0.75
ICA	3.9	29.0	4.0	29.1	2.56	0.34
Bulb	7.3	16.2	7.3	16.4	0.00	1.23

2.3. Computational modeling

2.3.1. Mathematical model

Blood was modeled as an incompressible fluid with density of 1,060 Kg/m^3 [3]. For a correct and complete description of hemodynamics, the appropriate viscosity model of blood must be chosen. Moreover, the different constitutive equations create a more pronounced variation in the radial velocity pattern than in the axial one [22]. So, in this study, to represent the shear-thinning behavior of blood, the non-Newtonian model was adopted and the viscosity was evaluated according to Carreau model [25], considering μ_0 of 0.056 Pa·s, μ_∞ of 0.0035 Pa·s, λ of 3.313 s, and n of 0.3568 [25]. This model was chosen because it coincides with power law model at low shear rates and with Casson and Newtonian models at high shear rate, so it is considered a suitable model [20].

Moreover, because the mean Reynolds number is about 300 [24], blood behavior in the carotid bifurcation was assumed as laminar and three-dimensional incompressible Navier–Stokes equations were used to numerically describe its motion:

$$\nabla \cdot u = 0 , \quad (1)$$

$$\rho(\partial u / \partial t) + \rho(u \cdot \nabla)u = \nabla \cdot [-p\mathrm{I} + \mu(\nabla u + (\nabla u)^T)] + F , \quad (2)$$

in which u represents the fluid velocity vector, p the pressure, μ the dynamic viscosity, ρ the density of blood, I the identity matrix, and F the volume force field.

2.3.2. Boundary conditions

As inlet boundary condition, pressure was chosen and applied to the CCA, whereas the velocity waveforms in ICA and ECA were assumed as outlet boundary conditions, considering in both cases a fully developed steady profile (Poiseuille distribution). The boundary conditions used in the sitting and in the standing situations are illustrated in Fig. 2.

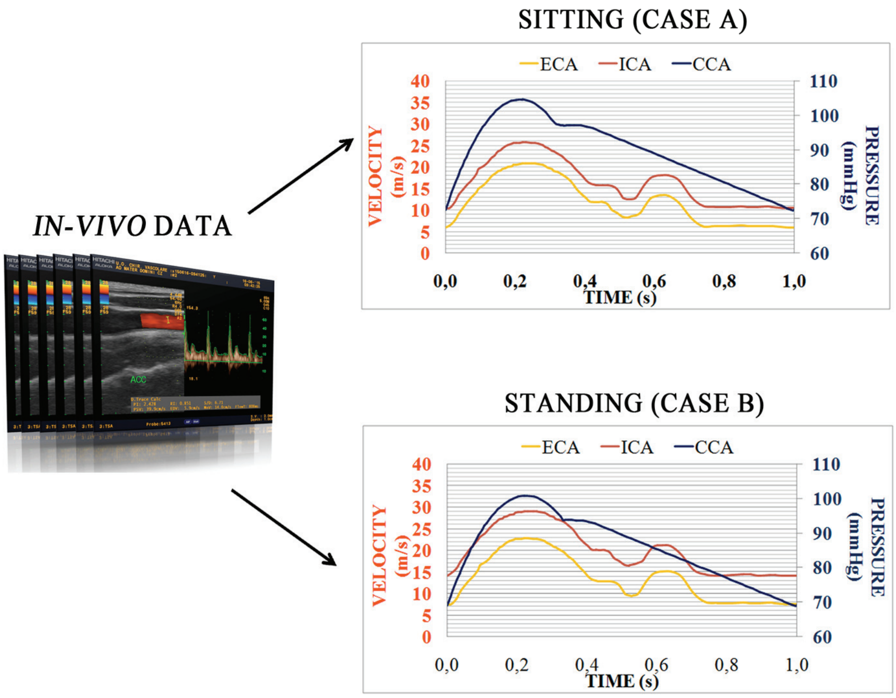

Fig. 2. Boundary conditions in sitting (case A) and in standing (case B) positions. Each behavior was obtained calculating the mean value for each time considering the cohort of volunteers

Since the aim of the study was to compare the hemodynamics in two sedentary conditions and since the wall elasticity behavior in these two situations is unknown, the elasticity of walls was neglected in order to perform this preliminary computational analysis. Thus, walls were approximated as rigid surfaces applying a no-slip boundary condition, as in other CFD studies [4], [6]. This assumption was also necessary to reduce the computational cost. Moreover, as reported by Malek et al. [15], atherosclerosis is correlated to the wall shear stress (WSS). The thresholds of different WSS parameters have been estimated in the carotid bifurcation considering rigid wall and fully developed entry flow [13]. In order to investigate the incidence of atherosclerotic events in sedentary conditions, we wanted to evaluate different parameters arising from WSS. So, also for this reason, the elasticity of vessels was not considered in this study.

2.3.3. Mechanical indicators

As reported by Malek et al. [15], the atherosclerosis and the shear stress generated at interface between blood and artery wall, known as the wall shear stress (WSS), are highly correlated. WSS can be evaluated as

$$\mathrm{WSS} = \sqrt{[(\tau_x)^2 + (\tau_y)^2 + (\tau_z)^2]} \tag{3}$$

where τ_x, τ_y and τ_z are the viscous stresses in x, y and z directions, respectively. Moreover, the same authors have indicated that the physiological level of WSS in arteries is 1.5–2 Pa and that values less than 0.4 Pa are considered as low [15]. WSS is a time-dependent variable. Therefore, the average value over one cardiac cycle (T) can be calculated, which is known as time average WSS (TAWSS), as

$$\mathrm{TAWSS} = 1/T \cdot \int_0^T |\,\mathrm{WSS}\,|\, dt\,. \tag{4}$$

If TAWSS is less than 1 Pa, intimal thickening occurs [24].

Another variable correlated to the WSS is the oscillatory shear index (OSI), a dimensionless measure that indicates areas with WSS vector oscillations: the zero value indicates that the flow is orderly and unidirectional and that there are no WSS variations, whereas 0.5 indicates a purely unsteady and chaotic flow (variations of 180°) with zero WSS [4]. OSI can be evaluated as

$$\mathrm{OSI} = 0.5 \cdot \left\{ 1 - \left[\left(\left| \int_0^T \mathrm{WSS}\,dt \right| \right) \Big/ \int_0^T |\,\mathrm{WSS}\,|\,dt \right] \right\}. \quad (5)$$

This mechanical indicator is a good predictive parameter of plaque site, as reported in [16]. TAWSS and OSI could be combined in the relative residence time (RRT) variable, expressed as

$$\mathrm{RRT} = [(1 - 2 \cdot \mathrm{OSI}) \cdot \mathrm{TAWSS}]^{-1} \quad (6)$$

that represents the residence time of particles near the wall. Thus, it can be considered as a stasis parameter.

Atherosclerosis plaque can arise when the flow is disturbed with low WSS and high OSI [16] and this area can be identified considering WSS $\leq$ 0.481 Pa, OSI $\geq$ 0.145 and RRT $\geq$ 2.944 Pa^{-1} [13].

2.3.4. Particle tracking (PT) modeling

Since thrombo-emboli arising from atherosclerotic lesions at the carotid artery bifurcation can cause stroke [4], the thrombi distribution was also investigated, using the particle tracking module, and specifically, Newton's second law of motion. Thrombi were modeled as particles with a diameter of 2 mm and a density of 1,117 $\mathrm{Kg/m^3}$ [19]. In particular, 10,000 non-interfering particles were released from a random point on the proximal cross section of the CCA in every cardiac cycle (we hypothesized that the release time coincides with the cardiac cycle of 1 s since a flow injection from the heart occurs every cardiac cycle).

A drag force, expressed according to the Stokes law, was applied in order to define the velocity field and the dynamic viscosity, which were the same expressed in the CFD model. Furthermore, the other types of force, such as Saffman Lift Force and Faxen correction due to pressure, are neglected since they do not significantly affect the thrombi trajectories [19].

As inlet boundary condition, the CFD velocity pattern was considered, whereas the outlets were modeled with the freeze condition in order to recover thrombi distribution and the velocity values at the contact instant that was made with the wall.

Furthermore, all carotid walls were considered as specularly reflecting surfaces. So, the bounce condition was applied, which allows the particle momentum to be conserved.

2.3.5. Simulation details

COMSOL 5.0 (COMSOL, Inc, Stockholm, Sweden), a finite-element-based commercial software package, was used to carry out the numerical simulations, for the post process and to visualize the results.

In order to obtain grid-independent solutions, with a good quality and accuracy and an effective computational cost, four meshes, all realized with four boundary layers and tetrahedral elements, were compared to identify the best one. More specifically, the continuity law was chosen to evaluate the mesh error [2], which can be expressed as

$$e = |\,Q_{\mathrm{exact}} - Q_{\mathrm{numerical}}\,| \cdot 100 / Q_{\mathrm{exact}} \quad (7)$$

in which

$$Q_{\mathrm{exact}} = Q_{\mathrm{ICA}} + Q_{\mathrm{ECA}} = Q_{CCA} \quad (8)$$

with $Q_{\mathrm{numerical}} = Q_{\mathrm{CCA}}$ being evaluated by means of the CFD analysis.

For each mesh, the error evaluated according to equation (7) and the simulation time were calculated both for the sitting condition and for the standing one. Later, the mean error and time values were estimated considering the two sedentary conditions and then these mean values were normalized. The results of this sensitivity analysis are illustrated in Fig. 3a, in which the optimum mesh of 190,000 elements was indicated and reported (Fig. 3b).

The direct solvers used by COMSOL are MUMPS, PARDISO and SPOOLES, which are more robust than the iterative solvers, return the same solution but differ in their speed. Since PARDISO is faster and can store the solution out-of-core, it was chosen to solve Navier–Stokes equations and the P1-P1 finite element method was adopted for the space discretization in the equations of blood motion: linear elements were used for velocity components and pressure field [2]. Regarding the time stepping, BDF method is more stable and versatile than Generalized alpha, thus it is preferred for CFD analysis. For this reason, this solver was adopted in the computational analysis considering a step of 0.001 s. Finally, since Generalized alpha is more accurate than BDF method, the Generalized alpha method was used for the time stepping of the particle tracking analysis with a step of 0.001 s, whereas the direct MUMPS default solver was used as general solver.

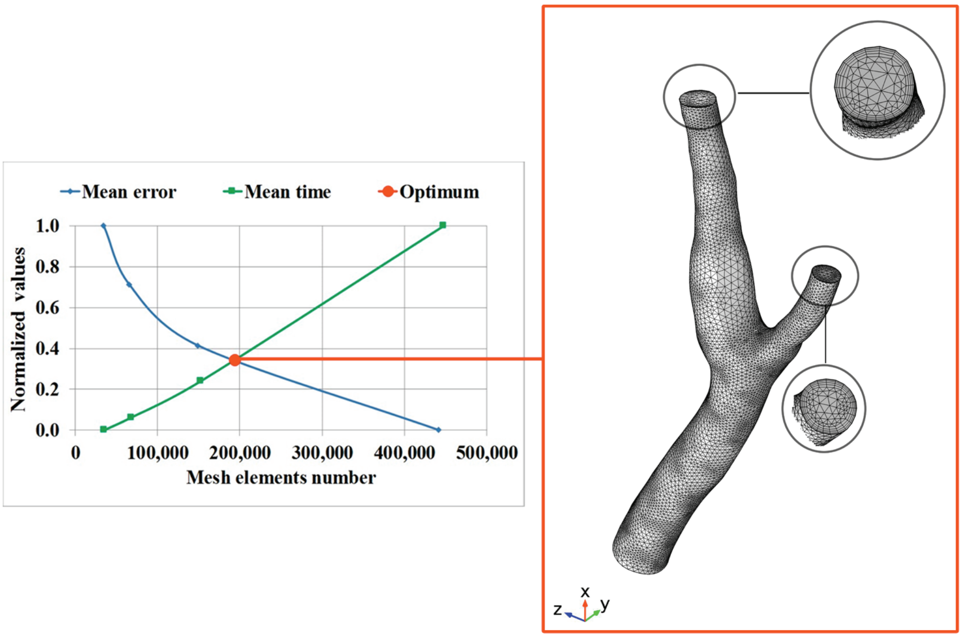

(a) (b)

Fig. 3. Mesh sensitivity analysis (a), in which the best mesh (optimum) was indicated, and the Final mesh of the 3D model with 190,000 elements (b)

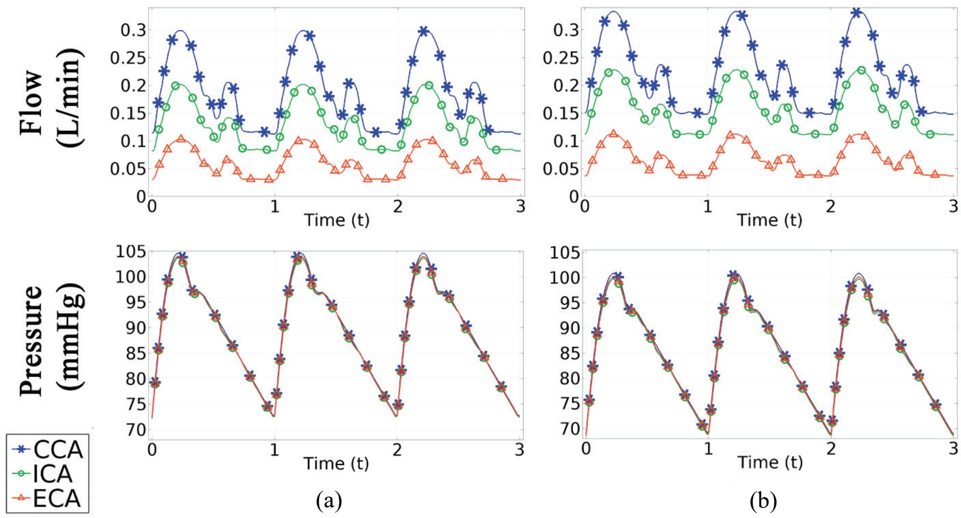

Fig. 4. Computational flow and pressure waveforms in sitting (case A) and in standing (case B) positions

For both CFD and PT simulations, three time cycles were simulated to eliminate the transitory initial effects due to the convergence process of both analyses and to guarantee stable solutions.

3. Results

In Fig. 4, flow and pressure waveforms in the sitting and in the standing positions, evaluated considering three cardiac cycles, are illustrated. The maximum flow rates are obtained in the standing position, in which the minimum pressure occurs. Moreover, the mean flow rates are 0.185 L/min in CCA, 0.128 L/min ICA, and 0.058 L/min in ECA in sitting condition and 0.220 L/min in CCA, 0.156 L/min ICA, and 0.066 L/min in ECA in standing condition. Regarding the pressure, it changes very little in the carotid bifurcation, with a maximum value of about 2 mmHg between CCA and ICA, both in sitting and in standing positions. For this reason, pressure could be considered as constant in the bifurcation in these two sedentary conditions.

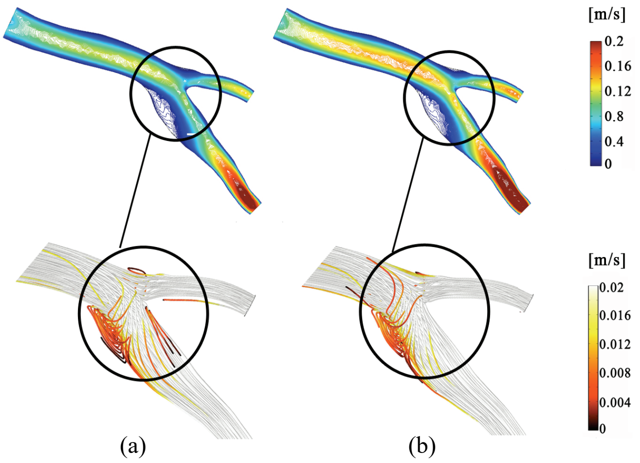

Fig. 5. Velocity pattern (up) and streamlines distribution (down) in the two positions: (a) sitting, (b) standing, during the diastolic deceleration phase, before the minimum flow rate ($t = 2.7$ s)

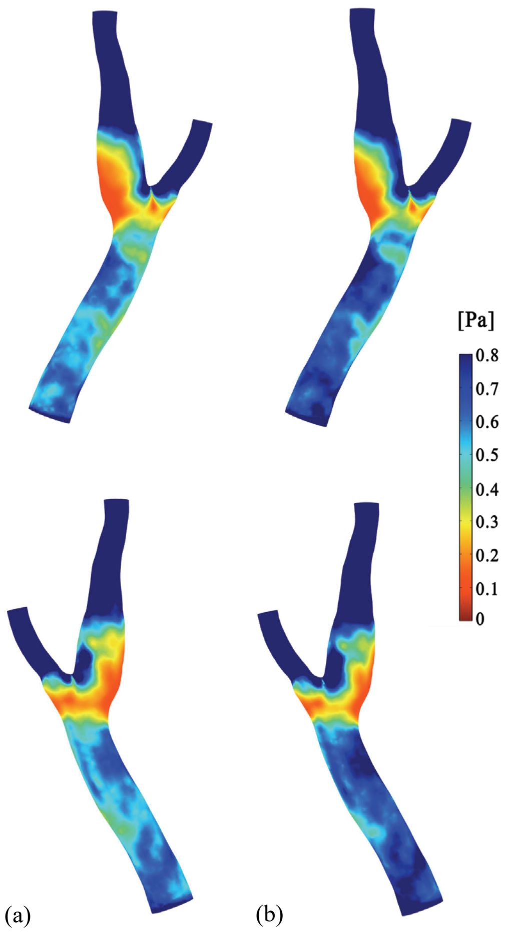

Fig. 6. TAWSS distribution in sitting (case A) and in standing (case B) positions, considering the frontal (up) and the posterior (down) views

In order to compare in detail the velocity patterns, the streamlines evaluated during the diastolic deceleration phase, before the minimum flow rate ($t = 2.7$ s), were analyzed. This comparison is reported in Fig. 5. In both cases, in correspondence of the bulb and at the emergence of ECA, velocity has a very low value, near 0 m/s. Furthermore, the region of bulb is characterized by high vorticity, especially in sitting position.

As reported by Malek et al. [15], the atherosclerosis is correlated to the WSS. So, to establish the worst sedentary position between sitting and standing, TAWSS, OSI and RRT were numerically evaluated and are illustrated in Figs. 6, 7 and 8, respectively. In both sedentary conditions, very low values of TAWSS, near 0 Pa were obtained in the bulb and in correspondence with ECA emergence. Moreover, low values (<0.481 Pa [13]) were also presented in the CCA trunk, especially in the sitting condition. The worst TAWSS profile was recorded in sitting position, in which values are lower than 17.2% with respect to the standing position. A similar situation occurs if the OSI distribution is considered (Fig. 7). Indeed, the flow is disturbed, with separations and recirculations (OSI ≈ 0.5) in the same bulb area as in the TAWSS distribution. Also, in this case, the worst situation is represented by the sitting condition, with value higher than 17.5% in respect to those obtained in standing position. Finally, the analysis of RRT distribution (Fig. 8) indicates that the area of bifurcation is characterized by stasis (RRT > 3 Pa^{-1}), both in correspondence of the bulb and ECA emergence, considering both sedentary conditions. Furthermore, this area is greater in the sitting position, in which also the CCA presents stagnant regions (red points): the RRT values in sitting position are over 21.2% with respect to the standing one. Finally, also the CCA trunk has stasis areas, especially in the sitting condition.

To investigate the motion of possible thrombi, the particle tracking was modeled and the results are illustrated in Table 3. Thrombi distribution in the outlet vessels, evaluated in the last phase of the last cardiac cycle, is greater in standing position, both in ICA and in ECA, whereas the percentage of particles which remain in the bifurcation is lower.

Table 3. Thrombi distribution in the outlet vessels in the last phase of each cardiac cycle. This value was evaluated considering that thrombi are released during every cardiac cycle (the release time coincides with the cardiac cycle of 1 s). Also the percentage of particles which remain in the bifurcation is reported

Sedentary behavior	ICA [%]	ECA [%]	Remain [%]
Sitting	32.10	27.67	40.23
Standing	36.64	30.85	32.51

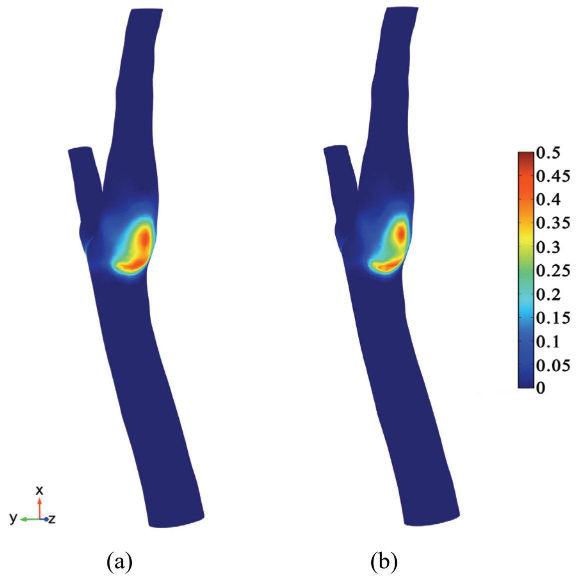

Fig. 7. OSI distribution in sitting (case A) and in standing (case B) positions

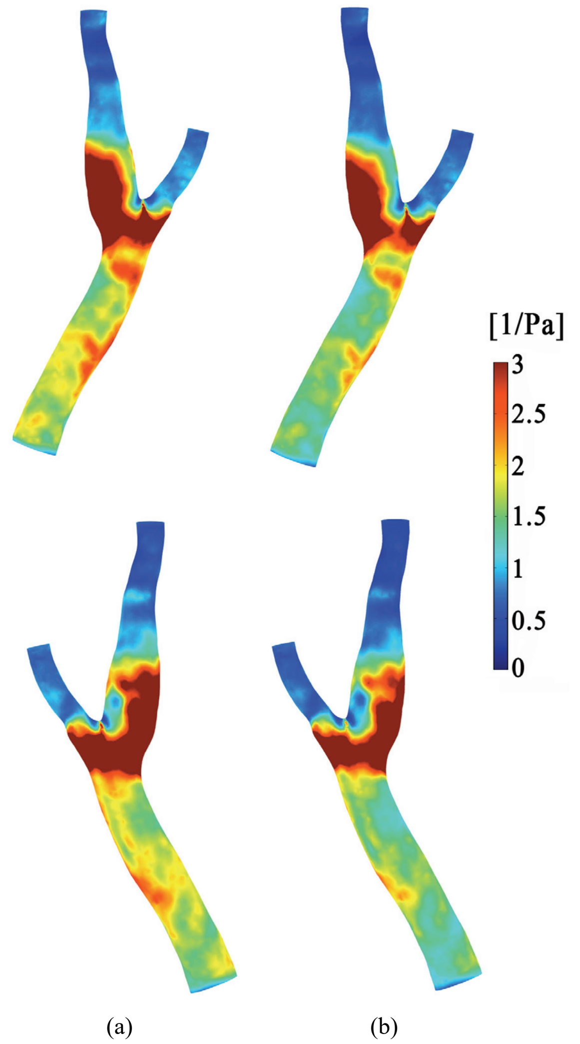

Fig. 8. RRT distribution in sitting (case A) and in standing (case B) positions, considering the frontal (up) and the posterior (down) views

4. Discussion

Sedentary lifestyle is a potent cause of vascular remodeling, leading to some alterations of the artery wall. On the other hand, increased physical activity seems to suppress the overall cardiovascular risk and hence curtails the progression of carotid atherosclerosis [8]. Sedentary lifestyle may be due to prolonged sitting or standing time, especially in particular working settings. Moreover, both sitting and standing positions seem to be involved in the carotid wall atherosclerosis. This computational study allows the carotid hemodynamic profiles in these two sedentary conditions to be compared in healthy subjects who spend most of their working time in those positions.

Since the geometry significantly alters the hemodynamics and, consequently, its parameters [6], a single patient-specific carotid bifurcation was used for the computational analysis in order to carry out a comparative study considering only the sedentary effects. Moreover, the rigid wall simplification was adopted because the wall elasticity behavior in these two situations is unknown and in order to make this comparative computational study more manageable, with a low computational cost. In addition, atherosclerosis is correlated to the WSS [15] and the thresholds of different WSS parameters have been estimated in the carotid bifurcation considering rigid wall and fully developed entry flow [13]. So, also for this second reason, the elasticity of vessels was neglected in this study, which has a minor effect on carotid bifurcation hemodynamics [13].

According to the law of continuity (1), the flow in CCA was numerically evaluated starting from the flow in ICA and ECA. So, as expected, all flows were higher in standing condition (Fig. 4), following the applied boundary conditions. Furthermore, since the carotid bifurcation is a small vessel (total length of about 6 cm), the maximum pressure variation due to the length was very low (about 2 mmHg), in both sedentary positions, which could be evaluated considering the hydrostatic pressure. Similar numerical results in the carotid bifurcation were obtained by [21], validating our CFD model.

In order to identify the worst hemodynamic profile due to the sedentary lifestyle and because atherosclerosis is highly correlated with the shear stress, TAWSS, OSI and RRT were considered as indicators of vascular wall dysfunction, as in similar works [16], [17], and numerically evaluated. These three parameters indicate that the bulb and the emergence of ECA are characterized by low velocity and WSS values, high OSI and, as a consequence, regions with chaotic and swirling flow, in which stasis occurs (high RRT). Similar hemodynamic results were found by other authors, both using a computational approach [17] and an *in vivo* investigation [16]. Indeed, these regions are the most susceptible to atherosclerosis, which occurs both in sitting and standing positions. Moreover, the sitting position mainly promotes atherosclerotic phenomena: TAWSS is less than 17.2% and OSI and RRT are greater than 17.5% and 21.2%, respectively.

Finally, the investigation of thrombi motion has shown that in the standing situation these particles have a high probability to move towards the brain and that a low percentage of thrombi remains in the bifurcation. The opposite situation occurs in the sitting position, in which the low velocities generate stasis areas, in which thrombi remain blocked.

Even though the purpose of this study is to compare the hemodynamic changes on carotid hemodynamics due to two types of sedentary lifestyle, it has a limitation: the approximation of rigid walls, neglecting the elasticity. So, a future perspective is to implement a fluid–structure interaction (FSI).

5. Conclusion

The carotid bifurcation is the region most relevant to the atherogenesis. Moreover, some risk factors have been identified as causes of atherosclerosis, such as the lifestyle, which could modify the hemodynamics. To investigate the effect of sedentary lifestyle in the carotid hemodynamics and to evaluate the incidence to the atherosclerotic events, we have carried out this computational study, comparing two sedentary conditions: prolonged sitting and prolonged standing. Our results have indicated that the worst hemodynamic pattern is generated in sitting position, in which stasis and swirling flow occurs in the bulb and in correspondence with the emergence of ECA. So, if a person spends much time in the sitting position, a high risk of plaque formation and, consequently, of stenosis could happen.

References

[1] Azhim A., Ueno A., Tanaka M., Akutagawa M., Kinouchi Y., *Evaluation of blood flow velocity envelope in common carotid artery for reference data*, Biomed Signal Proces, 2011, 6(2), 209–215, DOI: 10.1016/j.bspc.2010.11.002.

[2] Caruso M.V., Gramigna V., Rossi M., Serraino G.F., Renzulli A., Fragomeni G., *A computational fluid dynamics comparison between different outflow graft anastomosis locations of Left Ventricular Assist Device (LVAD) in a patient-specific aortic model*, International Journal for Numerical Methods in Biomedical Engineering, 2015, 31(2), DOI: 10.1002/cnm.2700.

[3] Cutnell J.D., Johnson K.W., *Physics*, Wiley, New York 1998.

[4] Dong J., Wong K.K., Tu J., *Hemodynamics analysis of patient-specific carotid bifurcation: A CFD model of downstream peripheral vascular impedance*, International Journal for Numerical Methods in Biomedical Engineering, 2013, 29(4), 476–491. DOI: 10.1002/cnm.2529

[5] Frangos S.G., Gahtan V., Sumpio B., *Localization of atherosclerosis: role of hemodynamics*, Arch. Surg. – Chicago, 1999, 134(10), 1142–1149, DOI: 10.1001/archsurg.134.10.1142.

[6] Friedman M.H., Deters O.J., Mark F.F., Bargeron C.B., Hutchins G.M., *Arterial geometry affects hemodynamics: a potential risk factor for atherosclerosis*, Atherosclerosis, 1983, 46(2), 225–231, DOI: 10.1016/0021-9150(83)90113-2.

[7] Gimbrone M.A., Topper J.N., Nagel T., Anderson K.R., Garcia-Cardeña G., *Endothelial dysfunction, hemodynamic forces, and atherogenesisa*, Ann. NY Acad. Sci., 2000, 902(1), 230–240, DOI: 10.1111/j.1749-6632.2000.tb06318.x.

[8] Kadoglou N.P.E., Iliadis F., Liapis C.D., *Exercise and carotid atherosclerosis*, European Journal of Vascular and Endovascular Surgery, 2008, 35(3), 264–272, DOI: 10.1016/j.ejvs.2007.08.022.

[9] Kozàkovà M., Palombo C., Morizzo C., Nolan J.J., Konrad T., Balkau B., *RISC Investigators, Effect of sedentary behaviour and vigorous physical activity on segment-specific carotid wall thickness and its progression in a healthy population*, Eur. Heart J., 2010, 31(12), 1511–1519.

[10] Krause N., Lynch J.W., Kaplan G.A., Cohen R.D., Salonen R., Salonen J.T., *Standing at work and progression of carotid atherosclerosis*, Scandinavian Journal of Work, Environment & Health, 2000, 227–236.

[11] Laufs U., Wassmann S., Czech T., Münzel T., Eisenhauer M., Böhm M., Nickenig G., *Physical inactivity increases oxidative stress, endothelial dysfunction, and atherosclerosis*, Arteriosclerosis, Thrombosis, and Vascular Biology, 2005, 25(4), 809–81, DOI: 10.1161/01.ATV.0000158311.24443.af

[12] Lee B.K., *Computational fluid dynamics in cardiovascular disease*, Korean Circulation Journal, 2011, 41(8), 423–430, DOI: 10.4070/kcj.2011.41.8.423.

[13] Lee S.W., Antiga L., Spence J.D., Steinman D.A., *Geometry of the carotid bifurcation predicts its exposure to disturbed flow*, Stroke, 2008, 39(8), 2341–2347.

[14] Lucas A.J., *Atherosclerosis*, Nature, 2000, 407, 233–41.

[15] Malek A.M., Alper S.L., Izumo S., *Hemodynamic shear stress and its role in atherosclerosis*, Jama, 1999, 282(21), 2035–2042, DOI: 10.1001/jama.282.21.2035.

[16] Markl M., Wegent F., Zech T., Bauer S., Strecker C., Harloff A., *In Vivo Wall Shear Stress Distribution in the Carotid Artery – Effect of Bifurcation Geometry, Internal Carotid Artery Stenosis, and Recanalization Therapy*, Circ. Cardiovasc. Imaging, 2010, 3, 647–655, DOI: 10.1161/CIRCIMAGING.110.958504

[17] Morbiducci U., Gallo D., Massai D., Consolo F., Ponzini R., Antiga L., Redaelli A., *Outflow conditions for image-based hemodynamic models of the carotid bifurcation: im-*

plications for indicators of abnormal flow, Journal of Biomechanical Engineering, 2010, 132(9), 091005, DOI: 10.1115/1.4001886.

[18] NEWCOMER S.C., SAUDER C.L., KUIPERS N.T., LAUGHLIN M.H., RAY C.A., *Effects of posture on shear rates in human brachial and superficial femoral arteries*, Am. J. Physiol.-Heart C, 2008, 294(4), H1833–H1839, DOI: 10.1152/ajpheart.01108.2007.

[19] OSORIO A.F., OSORIO R., CEBALLOS A., TRAN R., CLARK W., DIVO E.A., DECAMPLI W.M., *Computational fluid dynamics analysis of surgical adjustment of left ventricular assist device implantation to minimise stroke risk*, Comput. Method Biomec., 2013, 16(6), 622–638.

[20] RAZAVI A., SHIRANI E., SADEGHI M.R., *Numerical simulation of blood pulsatile flow in a stenosed carotid artery using different rheological models*, J. Biomech., 2011, 44(11), 2021–2030.

[21] REYMOND P., PERREN F., LAZEYRAS F., STERGIOPULOS N., *Patient-specific mean pressure drop in the systemic arterial tree, a comparison between 1-D and 3-D models*, J. Biomech., 2012, 45(15), 2499–2505. DOI: 10.1016/j.jbiomech.2012.07.020.

[22] SHIBESHI S.S., COLLINS W.E., *The rheology of blood flow in a branched arterial system*, Applied Rheology (Lappersdorf, Germany: Online), 2005, 15(6), 398.

[23] TU J., YEOH G.H., LIU C., *Computational fluid dynamics: a practical approach*, Butterworth–Heinemann, 2012.

[24] WOOTTON D.M., KU D.N., *Fluid mechanics of vascular systems, diseases, and thrombosis*, Annu. Rev. Biomed. Eng., 1999, 1(1), 299–329, DOI: 10.1146/annurev.bioeng.1.1.299.

[25] YILMAZ F., GUNDOGDU M.Y., *A critical review on blood flow in large arteries; relevance to blood rheology, viscosity models, and physiologic conditions*, Korea-Aust Rheol. J., 2008, 20(4), 197–211.